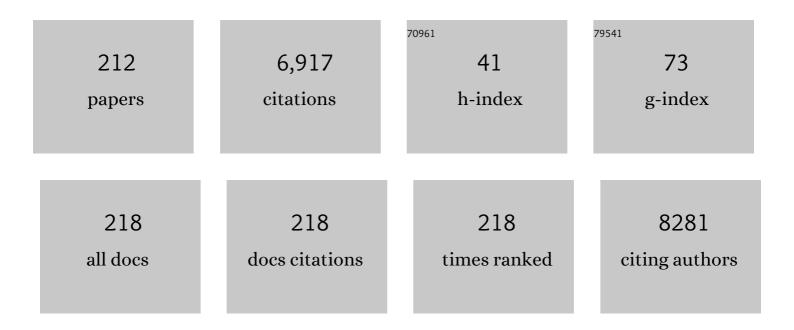
List of Publications by Year in descending order

Source: https://exaly.com/author-pdf/393429/publications.pdf Version: 2024-02-01



KADEN FOLED

#	Article	IF	CITATIONS
1	Disposable Coverslip for Rapid Throughput Screening of Malaria Using Attenuated Total Reflection Spectroscopy. Applied Spectroscopy, 2022, 76, 451-461.	1.2	5
2	Continuous rotary membrane emulsification for the production of sustainable Pickering emulsions. Chemical Engineering Science, 2022, 249, 117328.	1.9	6
3	Ab initio reconstruction of small angle scattering data for membrane proteins in copolymer nanodiscs. BBA Advances, 2022, 2, 100033.	0.7	0
4	Styrene–Maleic Acid Copolymer Nanodiscs to Determine the Shape of Membrane Proteins. Journal of Physical Chemistry B, 2022, 126, 1034-1044.	1.2	1
5	Fluorescent styrene maleic acid copolymers to facilitate membrane protein studies in lipid nanodiscs. Nanoscale, 2022, 14, 5689-5693.	2.8	3
6	Stable Cellulose Nanofibril Microcapsules from Pickering Emulsion Templates. Langmuir, 2022, 38, 3370-3379.	1.6	4
7	Membrane extraction with styrene-maleic acid copolymer results in insulin receptor autophosphorylation in the absence of ligand. Scientific Reports, 2022, 12, 3532.	1.6	5
8	The interaction of styrene maleic acid copolymers with phospholipids in Langmuir monolayers, vesicles and nanodiscs; a structural study. Journal of Colloid and Interface Science, 2022, 625, 220-236.	5.0	4
9	Production of sub-10 micrometre cellulose microbeads using isoporous membranes. , 2022, 2, 100024.		4
10	Neutron Diffraction Study of Indole Solvation in Deep Eutectic Systems of Choline Chloride, Malic Acid, and Water. Chemistry - A European Journal, 2022, 28, .	1.7	7
11	In situ X-ray reflectivity and GISAXS study of mesoporous silica films grown from sodium silicate solution precursors. Microporous and Mesoporous Materials, 2022, , 112018.	2.2	3
12	Interactions of water and amphiphiles with deep eutectic solvent nanostructures. Advances in Botanical Research, 2021, 97, 41-68.	0.5	12
13	Microstructural, Thermal, Crystallization, and Water Absorption Properties of Films Prepared from Neverâ€Dried and Freezeâ€Dried Cellulose Nanocrystals. Macromolecular Materials and Engineering, 2021, 306, 2000462.	1.7	3
14	Composite Hydrogel Spheroids Based on Cellulose Nanofibrils and Nanofibrous Chiral Coordination Polymer by Green Synthesis. Advanced Sustainable Systems, 2021, 5, 2000069.	2.7	2
15	Structural evolution of iron forming iron oxide in a deep eutectic-solvothermal reaction. Nanoscale, 2021, 13, 1723-1737.	2.8	14
16	Enzyme-Functionalized Cellulose Beads as a Promising Antimicrobial Material. Biomacromolecules, 2021, 22, 754-762.	2.6	17
17	Monovalent Salt and pH-Induced Gelation of Oxidised Cellulose Nanofibrils and Starch Networks: Combining Rheology and Small-Angle X-ray Scattering. Polymers, 2021, 13, 951.	2.0	3
18	Vesicular drug delivery for the treatment of topical disorders: current and future perspectives. Journal of Pharmacy and Pharmacology, 2021, 73, 1427-1441.	1.2	30

#	Article	IF	CITATIONS
19	Salt-Responsive Pickering Emulsions Stabilized by Functionalized Cellulose Nanofibrils. Langmuir, 2021, 37, 6864-6873.	1.6	15
20	Spin diffusion transfer difference (SDTD) NMR: An advanced method for the characterisation of water structuration within particle networks. Journal of Colloid and Interface Science, 2021, 594, 217-227.	5.0	6
21	Rheological modification of partially oxidised cellulose nanofibril gels with inorganic clays. PLoS ONE, 2021, 16, e0252660.	1.1	2
22	Physiochemical Changes to TTCF Ensilication Investigated Using Time-Resolved SAXS. AppliedChem, 2021, 1, 4-13.	0.2	0
23	Self-assembly of ionic and non-ionic surfactants in type IV cerium nitrate and urea based deep eutectic solvent. Journal of Chemical Physics, 2021, 155, 084902.	1.2	11
24	Synthesis, Properties, and Applications of Bio-Based Cyclic Aliphatic Polyesters. Biomacromolecules, 2021, 22, 3649-3667.	2.6	27
25	Long-Range Electrostatic Colloidal Interactions and Specific Ion Effects in Deep Eutectic Solvents. Journal of the American Chemical Society, 2021, 143, 14158-14168.	6.6	31
26	Bottom-up cubosome synthesis without organic solvents. Journal of Colloid and Interface Science, 2021, 601, 98-105.	5.0	9
27	Non-volatile conductive gels made from deep eutectic solvents and oxidised cellulose nanofibrils. Nanoscale Advances, 2021, 3, 2252-2260.	2.2	18
28	Deep eutectic solvents—The vital link between ionic liquids and ionic solutions. Journal of Chemical Physics, 2021, 155, 150401.	1.2	45
29	Development of Methodology to Investigate the Surface SMALPome of Mammalian Cells. Frontiers in Molecular Biosciences, 2021, 8, 780033.	1.6	3
30	Keratin–Chitosan Microcapsules via Membrane Emulsification and Interfacial Complexation. ACS Sustainable Chemistry and Engineering, 2021, 9, 16617-16626.	3.2	8
31	Recent progress in Pickering emulsions stabilised by bioderived particles. RSC Advances, 2021, 11, 39027-39044.	1.7	31
32	Influence of Aromatic Structure on the Thermal Behaviour of Lignin. Waste and Biomass Valorization, 2020, 11, 2863-2876.	1.8	17
33	Charge-driven interfacial gelation of cellulose nanofibrils across the water/oil interface. Soft Matter, 2020, 16, 357-365.	1.2	12
34	Cationic surfactants as a non-covalent linker for oxidised cellulose nanofibrils and starch-based hydrogels. Carbohydrate Polymers, 2020, 233, 115816.	5.1	18
35	Bacteriophage M13 Aggregation on a Microhole Poly(ethylene terephthalate) Substrate Produces an Anionic Current Rectifier: Sensitivity toward Anionic versus Cationic Guests. ACS Applied Bio Materials, 2020, 3, 512-521.	2.3	11
36	Multienzyme Cellulose Films as Sustainable and Self-Degradable Hydrogen Peroxide-Producing Material. Biomacromolecules, 2020, 21, 5315-5322.	2.6	4

#	Article	IF	CITATIONS
37	Structural and chemical heterogeneity in ancient glass probed using gas overcondensation, X-ray tomography, and solid-state NMR. Materials Characterization, 2020, 167, 110467.	1.9	5
38	Self-assembly of amphiphilic polyoxometalates for the preparation of mesoporous polyoxometalate-titania catalysts. Nanoscale, 2020, 12, 22245-22257.	2.8	14
39	Thermal resilience of ensilicated lysozyme <i>via</i> calorimetric and <i>in vivo</i> analysis. RSC Advances, 2020, 10, 29789-29796.	1.7	5
40	Deep eutectic solvent in water pickering emulsions stabilised by cellulose nanofibrils. RSC Advances, 2020, 10, 37023-37027.	1.7	8
41	Antagonistic mixing in micelles of amphiphilic polyoxometalates and hexaethylene glycol monododecyl ether. Journal of Colloid and Interface Science, 2020, 578, 608-618.	5.0	2
42	Morphology Modulation of Ionic Surfactant Micelles in Ternary Deep Eutectic Solvents. Journal of Physical Chemistry B, 2020, 124, 6004-6014.	1.2	26
43	Ensilicated tetanus antigen retains immunogenicity: in vivo study and time-resolved SAXS characterization. Scientific Reports, 2020, 10, 9243.	1.6	14
44	Filler size effect in an attractive fibrillated network: a structural and rheological perspective. Soft Matter, 2020, 16, 3303-3310.	1.2	12
45	Core–Shell Spheroidal Hydrogels Produced via Charge-Driven Interfacial Complexation. ACS Applied Polymer Materials, 2020, 2, 1213-1221.	2.0	2
46	Hydrophobization of Cellulose Nanocrystals for Aqueous Colloidal Suspensions and Gels. Biomacromolecules, 2020, 21, 1812-1823.	2.6	38
47	Toward Process-Resilient Lignin-Derived Activated Carbons for Hydrogen Storage Applications. ACS Sustainable Chemistry and Engineering, 2020, 8, 2186-2195.	3.2	33
48	Impact of wormlike micelles on nano and macroscopic structure of TEMPO-oxidized cellulose nanofibril hydrogels. Soft Matter, 2020, 16, 4887-4896.	1.2	7
49	Mesoporous Silica Formation Mechanisms Probed Using Combined Spin–Echo Modulated Small-Angle Neutron Scattering (SEMSANS) and Small-Angle Neutron Scattering (SANS). ACS Applied Materials & Interfaces, 2020, 12, 28461-28473.	4.0	15
50	Adsorption of a styrene maleic acid (SMA) copolymer-stabilized phospholipid nanodisc on a solid-supported planar lipid bilayer. Journal of Colloid and Interface Science, 2020, 574, 272-284.	5.0	9
51	In Situ Monitoring of Nanoparticle Formation during Iridium atalysed Oxygen Evolution by Realâ€Time Small Angle Xâ€Ray Scattering. ChemCatChem, 2019, 11, 5313-5321.	1.8	Ο
52	Assessing molecular simulation for the analysis of lipid monolayer reflectometry. Journal of Physics Communications, 2019, 3, 075001.	0.5	9
53	Temperature and concentration effects on decyltrimethylammonium micelles in water. Molecular Physics, 2019, 117, 3389-3397.	0.8	11
54	Mechanically robust cationic cellulose nanofibril 3D scaffolds with tuneable biomimetic porosity for cell culture. Journal of Materials Chemistry B, 2019, 7, 53-64.	2.9	22

#	Article	IF	CITATIONS
55	Structure and Properties of "Type IV―Lanthanide Nitrate Hydrate:Urea Deep Eutectic Solvents. ACS Sustainable Chemistry and Engineering, 2019, 7, 4932-4940.	3.2	52
56	Influence of levofloxacin and clarithromycin on the structure of DPPC monolayers. Biochimica Et Biophysica Acta - Biomembranes, 2019, 1861, 182994.	1.4	14
57	Bayesian determination of the effect of a deep eutectic solvent on the structure of lipid monolayers. Physical Chemistry Chemical Physics, 2019, 21, 6133-6141.	1.3	9
58	Processes associated with ionic current rectification at a 2D-titanate nanosheet deposit on a microhole poly(ethylene terephthalate) substrate. Journal of Solid State Electrochemistry, 2019, 23, 1237-1248.	1.2	12
59	Stability and behaviour in aqueous solutions of the anionic cubic silsesquioxane substituted with tetramethylammonium. Physical Chemistry Chemical Physics, 2019, 21, 6732-6742.	1.3	5
60	Application of Experimental Design to Hydrogen Storage: Optimisation of Lignin-Derived Carbons. Journal of Carbon Research, 2019, 5, 82.	1.4	6
61	Nano-encapsulated Escherichia coli Divisome Anchor ZipA, and in Complex with FtsZ. Scientific Reports, 2019, 9, 18712.	1.6	16
62	Nanostructure of the deep eutectic solvent/platinum electrode interface as a function of potential and water content. Nanoscale Horizons, 2019, 4, 158-168.	4.1	67
63	Understanding heat driven gelation of anionic cellulose nanofibrils: Combining saturation transfer difference (STD) NMR, small angle X-ray scattering (SAXS) and rheology. Journal of Colloid and Interface Science, 2019, 535, 205-213.	5.0	32
64	An introduction to classical molecular dynamics simulation for experimental scattering users. Journal of Applied Crystallography, 2019, 52, 665-668.	1.9	3
65	Influence of Poly(styrene- <i>co</i> -maleic acid) Copolymer Structure on the Properties and Self-Assembly of SMALP Nanodiscs. Biomacromolecules, 2018, 19, 761-772.	2.6	57
66	Unravelling cationic cellulose nanofibril hydrogel structure: NMR spectroscopy and small angle neutron scattering analyses. Soft Matter, 2018, 14, 255-263.	1.2	27
67	Codelivery of a cytotoxin and photosensitiser <i>via</i> a liposomal nanocarrier: a novel strategy for light-triggered cytosolic release. Nanoscale, 2018, 10, 20366-20376.	2.8	23
68	Alcohol induced gelation of TEMPO-oxidized cellulose nanofibril dispersions. Soft Matter, 2018, 14, 9243-9249.	1.2	19
69	Editorial overview: Going small for big impact. Current Opinion in Green and Sustainable Chemistry, 2018, 12, A1-A2.	3.2	0
70	An acid-compatible co-polymer for the solubilization of membranes and proteins into lipid bilayer-containing nanoparticles. Nanoscale, 2018, 10, 10609-10619.	2.8	91
71	TEMPO-oxidised cellulose nanofibrils; probing the mechanisms of gelation <i>via</i> small angle X-ray scattering. Physical Chemistry Chemical Physics, 2018, 20, 16012-16020.	1.3	41
72	Towards Truly Stealth Nanodiscs. Biophysical Journal, 2018, 114, 236a.	0.2	0

#	Article	IF	CITATIONS
73	Surfactant controlled zwitterionic cellulose nanofibril dispersions. Soft Matter, 2018, 14, 7793-7800.	1.2	16
74	Pickering emulsions stabilized by naturally derived or biodegradable particles. Current Opinion in Green and Sustainable Chemistry, 2018, 12, 83-90.	3.2	121
75	Counterion binding alters surfactant self-assembly in deep eutectic solvents. Physical Chemistry Chemical Physics, 2018, 20, 13952-13961.	1.3	30
76	Self-assembly and surface behaviour of pure and mixed zwitterionic amphiphiles in a deep eutectic solvent. Soft Matter, 2018, 14, 5525-5536.	1.2	30
77	pylj: A teaching tool for classical atomistic simulation. The Journal of Open Source Education, 2018, 1, 19.	0.2	2
78	Formation of Ordered Mesoporous Thin Films Through Templating. , 2018, , 917-983.		3
79	Model-dependent Small-angle Scattering for the Study of Complex Organic Materials. Current Organic Chemistry, 2018, 22, 750-757.	0.9	0
80	Deep eutectic-solvothermal synthesis of nanostructured ceria. Nature Communications, 2017, 8, 14150.	5.8	122
81	Freeâ€Standing Phytantriol Q ²²⁴ Cubicâ€Phase Films: Resistivity Monitoring and Switching. ChemElectroChem, 2017, 4, 1172-1180.	1.7	11
82	Thermal stability, storage and release of proteins with tailored fit in silica. Scientific Reports, 2017, 7, 46568.	1.6	36
83	Sulfur-Doped Cubic Mesostructured Titania Films for Use as a Solar Photocatalyst. Journal of Physical Chemistry C, 2017, 121, 9929-9937.	1.5	21
84	The Effect of Water upon Deep Eutectic Solvent Nanostructure: An Unusual Transition from Ionic Mixture to Aqueous Solution. Angewandte Chemie, 2017, 129, 9914-9917.	1.6	59
85	The Effect of Water upon Deep Eutectic Solvent Nanostructure: An Unusual Transition from Ionic Mixture to Aqueous Solution. Angewandte Chemie - International Edition, 2017, 56, 9782-9785.	7.2	497
86	Coarse-grained empirical potential structure refinement: Application to a reverse aqueous micelle. Biochimica Et Biophysica Acta - General Subjects, 2017, 1861, 1652-1660.	1.1	11
87	Protein conformation in pure and hydrated deep eutectic solvents. Physical Chemistry Chemical Physics, 2017, 19, 8667-8670.	1.3	97
88	Decyltrimethylammonium Bromide Micelles in Acidic Solutions: Counterion Binding, Water Structuring, and Micelle Shape. Langmuir, 2017, 33, 262-271.	1.6	11
89	Resilience of Malic Acid Natural Deep Eutectic Solvent Nanostructure to Solidification and Hydration. Journal of Physical Chemistry B, 2017, 121, 7473-7483.	1.2	122
90	Innenrücktitelbild: The Effect of Water upon Deep Eutectic Solvent Nanostructure: An Unusual Transition from Ionic Mixture to Aqueous Solution (Angew. Chem. 33/2017). Angewandte Chemie, 2017, 129, 10131-10131.	1.6	1

#	Article	IF	CITATIONS
91	Surfactant–Solvent Interaction Effects on the Micellization of Cationic Surfactants in a Carboxylic Acid-Based Deep Eutectic Solvent. Langmuir, 2017, 33, 14304-14314.	1.6	56
92	Azulene–boronate esters: colorimetric indicators for fluoride in drinking water. Chemical Communications, 2017, 53, 12580-12583.	2.2	65
93	Microwave-assisted deep eutectic-solvothermal preparation of iron oxide nanoparticles for photoelectrochemical solar water splitting. Journal of Materials Chemistry A, 2017, 5, 16189-16199.	5.2	40
94	Formation of Ordered Mesoporous Thin Films Through Templating. , 2017, , 1-67.		0
95	Micellization of alkyltrimethylammonium bromide surfactants in choline chloride:glycerol deep eutectic solvent. Physical Chemistry Chemical Physics, 2016, 18, 33240-33249.	1.3	53
96	Micelle structure in a deep eutectic solvent: a small-angle scattering study. Physical Chemistry Chemical Physics, 2016, 18, 14063-14073.	1.3	55
97	A neutron scattering and modelling study of aqueous solutions of tetramethylammonium and tetrapropylammonium bromide. Physical Chemistry Chemical Physics, 2016, 18, 11193-11201.	1.3	24
98	Outset of the Morphology of Nanostructured Silica Particles during Nucleation Followed by Ultrasmall-Angle X-ray Scattering. Langmuir, 2016, 32, 5162-5172.	1.6	14
99	Evidence of Lipid Exchange in Styrene Maleic Acid Lipid Particle (SMALP) Nanodisc Systems. Langmuir, 2016, 32, 11845-11853.	1.6	38
100	Ibuprofen delivery into and through the skin from novel oxidized cellulose-based gels and conventional topical formulations. International Journal of Pharmaceutics, 2016, 514, 238-243.	2.6	29
101	Insights into the Influence of Solvent Polarity on the Crystallization of Poly(ethylene oxide) Spin-Coated Thin Films viain SituGrazing Incidence Wide-Angle X-ray Scattering. Macromolecules, 2016, 49, 4579-4586.	2.2	31
102	Langmuir monolayers composed of single and double tail sulfobetaine lipids. Journal of Colloid and Interface Science, 2016, 474, 190-198.	5.0	15
103	Liquid structure of the choline chloride-urea deep eutectic solvent (reline) from neutron diffraction and atomistic modelling. Green Chemistry, 2016, 18, 2736-2744.	4.6	395
104	Kinetic Influence of Siliceous Reactions on Structure Formation of Mesoporous Silica Formed via the Co-Structure Directing Agent Route. Journal of Physical Chemistry C, 2016, 120, 3814-3821.	1.5	7
105	Encapsulated membrane proteins: A simplified system for molecular simulation. Biochimica Et Biophysica Acta - Biomembranes, 2016, 1858, 2549-2557.	1.4	25
106	Atomistic modelling of scattering data in the Collaborative Computational Project for Small Angle Scattering (CCP-SAS). Journal of Applied Crystallography, 2016, 49, 1861-1875.	1.9	67
107	Convection-Enhanced Delivery of Carboplatin PLGA Nanoparticles for the Treatment of Glioblastoma. PLoS ONE, 2015, 10, e0132266.	1.1	67
108	Gas sensing using porous materials for automotive applications. Chemical Society Reviews, 2015, 44, 4290-4321.	18.7	406

#	Article	IF	CITATIONS
109	Small Angle Neutron Scattering Studies on the Internal Structure of Poly(lactide- <i>co</i> -glycolide)- <i>block</i> -poly(ethylene glycol) Nanoparticles as Drug Delivery Vehicles. Biomacromolecules, 2015, 16, 457-464.	2.6	25
110	Combining wide-angle and small-angle scattering to study colloids and self-assembly. Current Opinion in Colloid and Interface Science, 2015, 20, 227-234.	3.4	8
111	Interactions between quaternary ammonium surfactants and polyethylenimine at high pH in film forming systems. Journal of Colloid and Interface Science, 2015, 449, 286-296.	5.0	7
112	Intrinsically Microporous Polymer Retains Porosity in Vacuum Thermolysis to Electroactive Heterocarbon. Langmuir, 2015, 31, 12300-12306.	1.6	25
113	Surfactant Behavior of Sodium Dodecylsulfate in Deep Eutectic Solvent Choline Chloride/Urea. Langmuir, 2015, 31, 12894-12902.	1.6	105
114	Ordered Mesoporous Particles in Titania Films with Hierarchical Structure as Scattering Layers in Dye-Sensitized Solar Cells. Journal of Physical Chemistry C, 2015, 119, 22552-22559.	1.5	22
115	Structural analysis of a nanoparticle containing a lipid bilayer used for detergent-free extraction of membrane proteins. Nano Research, 2015, 8, 774-789.	5.8	161
116	Free-Standing High Surface Area Titania Films Grown at the Air–Water Interface. Journal of Physical Chemistry C, 2014, 118, 26641-26648.	1.5	0
117	Orientation specific deposition of mesoporous particles. APL Materials, 2014, 2, 113305.	2.2	5
118	Voltammetric optimisation of TEMPO-mediated oxidations at cellulose fabric. Green Chemistry, 2014, 16, 3322-3327.	4.6	29
119	Water-Responsive Internally Structured Polymer–Surfactant Films on Solid Surfaces. Langmuir, 2014, 30, 12525-12531.	1.6	10
120	Controlling Interfacial Film Formation in Mixed Polymer–Surfactant Systems by Changing the Vapor Phase. Langmuir, 2014, 30, 9991-10001.	1.6	6
121	NMR cryoporometry characterisation studies of the relation between drug release profile and pore structural evolution of polymeric nanoparticles. International Journal of Pharmaceutics, 2014, 469, 146-158.	2.6	27
122	Partially Oxidised Cellulose Nanofibril Gels for Rheology Modification. Acta Crystallographica Section A: Foundations and Advances, 2014, 70, C1320-C1320.	0.0	1
123	Self-assembly and phase behaviour of PEI : cationic surfactant aqueous mixtures forming mesostructured films at the air/solution interface. Soft Matter, 2013, 9, 4003.	1.2	11
124	Formation of low density hydrous iron oxide via conformal transformation of MIL-53(Fe). Chemical Communications, 2013, 49, 10593.	2.2	3
125	Insights into the Role of Polymer-Surfactant Complexes in Drug Solubilisation/Stabilisation During Drug Release from Solid Dispersions. Pharmaceutical Research, 2013, 30, 290-302.	1.7	83
126	Probing hysteresis during sorption of cyclohexane within mesoporous silica using NMR cryoporometry and relaxometry. Journal of Colloid and Interface Science, 2013, 398, 168-175.	5.0	8

#	Article	IF	CITATIONS
127	Robust Ordered Cubic Mesostructured Polymer/Silica Composite Films Grown at the Air/Water Interface. Langmuir, 2013, 29, 4148-4158.	1.6	9
128	Facile synthesis of crack-free metal–organic framework films on alumina by a dip-coating route in the presence of polyethylenimine. Journal of Materials Chemistry A, 2013, 1, 5497.	5.2	41
129	Formation of mesostructured thin films at the air–liquid interface. Chemical Society Reviews, 2013, 42, 3765-3776.	18.7	38
130	Synthesis and post-synthetic modification of MIL-101(Cr)-NH2via a tandem diazotisation process. Chemical Communications, 2012, 48, 12053.	2.2	166
131	Silica–Surfactant–Polyelectrolyte Film Formation: Evolution in the Subphase. Langmuir, 2012, 28, 8337-8347.	1.6	12
132	Facile synthesis of metal–organic framework films via in situ seeding of nanoparticles. Chemical Communications, 2012, 48, 4965.	2.2	27
133	Probing the impact of advanced melting and advanced adsorption phenomena on the accuracy of pore size distributions from cryoporometry and adsorption using NMR relaxometry and diffusometry. Journal of Colloid and Interface Science, 2012, 385, 183-192.	5.0	17
134	Formation of shear thinning gels from partially oxidised cellulose nanofibrils. Green Chemistry, 2012, 14, 300-303.	4.6	53
135	Control of mesostructure in self-assembled polymer/surfactant films by rational micelle design. Soft Matter, 2012, 8, 3357.	1.2	11
136	Hydrothermal core–shell carbon nanoparticle films: thinning the shell leads to dramatic pH response. Physical Chemistry Chemical Physics, 2012, 14, 15860.	1.3	9
137	The role of protein hydrophobicity in thionin–phospholipid interactions: a comparison of α1 and α2-purothionin adsorbed anionic phospholipid monolayers. Physical Chemistry Chemical Physics, 2012, 14, 13569.	1.3	15
138	Mesoporous Silica Sputterâ€Coated onto ITO: Electrochemical Processes, Ion Permeability, and Gold Deposition Through NanoPores. Electroanalysis, 2012, 24, 1296-1305.	1.5	5
139	Growth-collapse mechanism of PEI-CTAB films at the air–water interface. Soft Matter, 2011, 7, 11125.	1.2	13
140	Size-controlled synthesis of MIL-101(Cr) nanoparticles with enhanced selectivity for CO2 over N2. CrystEngComm, 2011, 13, 6916.	1.3	128
141	Mesoporous titanium dioxide films using partially fluorinated surfactant templates in ethanol. Journal of Materials Chemistry, 2011, 21, 14062.	6.7	3
142	Atomistic Structure of a Micelle in Solution Determined by Wide <i>Q</i> -Range Neutron Diffraction. Journal of the American Chemical Society, 2011, 133, 16524-16536.	6.6	66
143	Tuning percolation speed in layer-by-layer assembled polyaniline–nanocellulose composite films. Journal of Solid State Electrochemistry, 2011, 15, 2675-2681.	1.2	24
144	DNA Binding to Zwitterionic Model Membranes. Langmuir, 2010, 26, 4965-4976.	1.6	49

#	Article	IF	CITATIONS
145	Boronic aciddendrimerreceptor modified nanofibrillar cellulose membranes. Journal of Materials Chemistry, 2010, 20, 588-594.	6.7	37
146	Microwave-electrochemical formation of colloidal zinc oxide at fluorine doped tin oxide electrodes. Electrochimica Acta, 2010, 55, 7909-7915.	2.6	10
147	Ultrathin Carbon Film Electrodes from Vacuum arbonised Cellulose Nanofibril Composite. Electroanalysis, 2010, 22, 619-624.	1.5	19
148	Assembly of nonionic–anionic co-surfactants to template mesoporous silica vesicles with hierarchical structures. Microporous and Mesoporous Materials, 2010, 131, 21-27.	2.2	17
149	Studies of structure–transport relationships in biodegradable polymer microspheres for drug delivery using NMR cryodiffusometry. Chemical Engineering Science, 2010, 65, 611-625.	1.9	9
150	Association of Titania with Nonionic Block Copolymers in Ethanol: The Early Stages of Templating and Film Formation. Chemistry of Materials, 2010, 22, 4579-4590.	3.2	7
151	Electrochemically Active Mercury Nanodroplets Trapped in a Carbon Nanoparticle–Chitosan Matrix. Electroanalysis, 2009, 21, 261-266.	1.5	21
152	Multiple thin film formation from dilute mixtures of polyethyleneimine (PEI) and cetyltrimethylammonium bromide (CTAB). Journal of Colloid and Interface Science, 2009, 339, 495-501.	5.0	8
153	Nonequilibrium Phase Transformations at the Airâ^'Liquid Interface. Langmuir, 2009, 25, 12177-12184.	1.6	16
154	Self-Assembled Films Formed at the Air–Water Interface from CTAB/SDS Mixtures with Water-Soluble Polymers. Langmuir, 2009, 25, 4047-4055.	1.6	15
155	Free-Standing Ordered Mesoporous Silica Films Synthesized with Surfactantâ^'Polyelectrolyte Complexes at the Air/Water Interface. Chemistry of Materials, 2009, 21, 1221-1231.	3.2	36
156	Underpotential surface reduction of mesoporous CeO2 nanoparticle films. Journal of Solid State Electrochemistry, 2008, 12, 1541-1548.	1.2	7
157	Fundamental studies of gas sorption within mesopores situated amidst an inter-connected, irregular network. Adsorption, 2008, 14, 289-307.	1.4	16
158	Incorporation of sparingly soluble species in mesostructured surfactant–polymer films. Journal of Colloid and Interface Science, 2008, 317, 585-592.	5.0	10
159	Chemically surface-modified carbon nanoparticle carrier for phenolic pollutants: Extraction and electrochemical determination of benzophenone-3 and triclosan. Analytica Chimica Acta, 2008, 616, 28-35.	2.6	64
160	Determination of the percolation properties and pore connectivity for mesoporous solids using NMR cryodiffusometry. Chemical Engineering Science, 2008, 63, 1929-1940.	1.9	37
161	Direct reversible voltammetry and electrocatalysis with surface-stabilised Fe2O3 redox states. Electrochemistry Communications, 2008, 10, 1773-1776.	2.3	38
162	Thin-Film Modified Electrodes with Reconstituted Celluloseâ^'PDDAC Films for the Accumulation and Detection of Triclosan. Journal of Physical Chemistry C, 2008, 112, 2660-2666.	1.5	56

#	Article	IF	CITATIONS
163	Liquid Crystal Codendrimers with a Statistical Distribution of Phenolic and Mesogenic Groups: Behavior as Langmuir and Langmuirâ `Blodgett Films. Langmuir, 2008, 24, 11082-11088.	1.6	12
164	Evolution of non-ionic surfactant-templated silicate films at the air–liquid interface. Journal of Materials Chemistry, 2008, 18, 1222.	6.7	11
165	Interactions and film formation in polyethylenimine–cetyltrimethylammonium bromide aqueous mixtures at low surfactant concentration. Soft Matter, 2007, 3, 747-753.	1.2	25
166	Formation of robust, free-standing nanostructured membranes from catanionic surfactant mixtures and hydrophilic polymers. Chemical Communications, 2007, , 1068-1070.	2.2	19
167	Macroscopic, Mesostructured Cationic Surfactant/Neutral Polymer Films:Â Structure and Cross-Linking. Langmuir, 2007, 23, 4589-4598.	1.6	16
168	Langmuir–Blodgett Deposited Monolayers of Silicalite-1 Seeds for Secondary Growth of Continuous Zeolite Films. Chemistry of Materials, 2007, 19, 5806-5808.	3.2	32
169	Mesoporous Silver Films from Dilute Mixed-Surfactant Solutions by Using Dip-Coating. Advanced Materials, 2007, 19, 1506-1509.	11.1	21
170	Electro-deposition of thin cellulose films at boron-doped diamond substrates. Electrochemistry Communications, 2007, 9, 42-48.	2.3	10
171	Layer-by-layer deposition of open-pore mesoporous TiO2-Nafion® film electrodes. Journal of Solid State Electrochemistry, 2007, 11, 1109-1117.	1.2	16
172	Nanoscum: solid nanostructured films at the air–water interface. Soft Matter, 2006, 2, 284.	1.2	11
173	Effect of Micelle Composition on the Formation of Surfactant-Templated Polymer Films. Journal of Physical Chemistry B, 2006, 110, 5330-5336.	1.2	9
174	Microcalorimetric Study of Ammonia Chemisorption on H3PW12O40Supported onto Mesoporous Synthetic Carbons and SBA-15. Langmuir, 2006, 22, 7664-7671.	1.6	11
175	Using Nano-Cast Model Porous Media and Integrated Gas Sorption to Improve Fundamental Understanding and Data Interpretation in Mercury Porosimetry. Particle and Particle Systems Characterization, 2006, 23, 82-93.	1.2	13
176	Formation of mesostructured thin films at the air/water interface. Thin Solid Films, 2006, 495, 2-10.	0.8	14
177	Synthesis, Assembly and Reactivity of Metallic Nanorods. , 2005, , 285-307.		1
178	Current Understanding of Formation Mechanisms in Surfactant-Templated Materials. ChemInform, 2005, 36, no.	0.1	0
179	Current Understanding of Formation Mechanisms in Surfactant-Templated Materials. Australian Journal of Chemistry, 2005, 58, 627.	0.5	46
180	Thin Films of Polyethylenimine and Alkyltrimethylammonium Bromides at the Air/Water Interface. Macromolecules, 2005, 38, 8785-8794.	2.2	41

#	Article	IF	CITATIONS
181	Modeling the Fractal Growth of Templated, Mesoporous Silica Films. Journal of Physical Chemistry B, 2005, 109, 6294-6303.	1.2	4
182	An Experimental Study of Gas Adsorption on Fractal Surfaces. Langmuir, 2005, 21, 2281-2292.	1.6	72
183	Self-Organization of Metallic Nanorods into Liquid Crystalline Arrays. , 2005, , 515-524.		0
184	Formation of surfactant–silica mesophase films at a silica interface. , 2004, , 169-174.		0
185	Nanocasting of novel, designer-structured catalyst supports. Chemical Engineering Science, 2004, 59, 5113-5120.	1.9	11
186	Soap and sand: construction tools for nanotechnology. Philosophical Transactions Series A, Mathematical, Physical, and Engineering Sciences, 2004, 362, 2635-2651.	1.6	15
187	Measurement of the Adsorption of Cytochrome c onto the External Surface of a Thin-Film Mesoporous Silicate by Ellipsometry. Langmuir, 2004, 20, 532-536.	1.6	24
188	Humidity and Temperature Effects on CTAB-Templated Mesophase Silicate Films at the Airâ^'Liquid Interface. Langmuir, 2004, 20, 10679-10684.	1.6	11
189	Preparation and characterisation of chemisorbents based on heteropolyacids supported on synthetic mesoporous carbons and silica. Catalysis Today, 2003, 81, 611-621.	2.2	79
190	Formation of CTAB-templated mesophase silicate films from acidic solutions. Microporous and Mesoporous Materials, 2003, 62, 165-175.	2.2	29
191	Characterization of the Structure of Mesoporous Thin Films Grown at the Air/Water Interface Using X-ray Surface Techniques. Langmuir, 2003, 19, 2639-2642.	1.6	19
192	Spontaneous free-standing nanostructured film growth in polyelectrolyte-surfactant systems. Chemical Communications, 2003, , 1724.	2.2	34
193	Concentration-Dependent Formation Mechanisms in Mesophase Silicaâ^'Surfactant Films. Langmuir, 2002, 18, 9838-9844.	1.6	42
194	The effect of surface texture on total reflection of neutrons and X-rays from modified interfaces. Physical Chemistry Chemical Physics, 2002, 4, 2379-2386.	1.3	3
195	Liquid crystalline assemblies of ordered gold nanorods. Journal of Materials Chemistry, 2002, 12, 2909-2912.	6.7	191
196	Structural Evolution of Surfactantâ^'Silica Film-Forming Solutions, Investigated Using Small-Angle Neutron Scattering. Chemistry of Materials, 2002, 14, 4292-4299.	3.2	31
197	The Influence of Mercury Contact Angle, Surface Tension, and Retraction Mechanism on the Interpretation of Mercury Porosimetry Data. Journal of Colloid and Interface Science, 2002, 250, 175-190.	5.0	91
198	Growth and characterization of mesoporous silica films. International Reviews in Physical Chemistry, 2001, 20, 387-466.	0.9	72

#	Article	lF	CITATIONS
199	The effect of hydrogen on the morphology of n-type silicon electrodes under electrochemical conditions. Physical Chemistry Chemical Physics, 2001, 3, 5559-5566.	1.3	6
200	Structural studies on surfactant-templated silica films grown at the air/water interface. Microporous and Mesoporous Materials, 2001, 44-45, 661-670.	2.2	35
201	In situ Brewster angle microscopy and surface pressure studies on the interfacial growth of mesostructured silica thin films. Chemical Communications, 2000, , 773-774.	2.2	13
202	Silica Gels with Tunable Nanopores through Templating of the L3Phase. Langmuir, 2000, 16, 398-406.	1.6	37
203	Preparation dependent stability of pure silica MCMâ€41. Journal of Materials Chemistry, 1999, 9, 2611-2615.	6.7	30
204	Shear and salt effects on the structure of MCM-41 synthesis gels. Journal of the Chemical Society, Faraday Transactions, 1998, 94, 1287-1291.	1.7	12
205	Small-Angle Neutron Scattering Studies on the Mesoporous Molecular Sieve MCM-41. Journal of Physical Chemistry B, 1998, 102, 3676-3683.	1.2	67
206	Diffuse wall structure and narrow mesopores in highly crystalline MCM-41 materials studied by X-ray diffraction. Journal of the Chemical Society, Faraday Transactions, 1997, 93, 199-202.	1.7	104
207	Structure and dynamics of hydrogen sorption in mesoporous MCM-41. Journal of the Chemical Society, Faraday Transactions, 1997, 93, 1667-1674.	1.7	45
208	Further Improvements in the Long-Range Order of MCM-41 Materials. Chemistry of Materials, 1997, 9, 1226-1233.	3.2	111
209	Small angle X-ray scattering from MCM-41 and its synthesis gels: optimisation of the synthesis parameters. Colloids and Surfaces A: Physicochemical and Engineering Aspects, 1995, 102, 213-230.	2.3	36
210	Room-temperature formation of molecular sieve MCM-41. Journal of the Chemical Society Chemical Communications, 1995, , 155.	2.0	49
211	Cellulose Microbeads: Toward the Controlled Release of Nutrients to Plants. ACS Agricultural Science and Technology, 0, , .	1.0	5
212	Efficient Encapsulation and Controlled Release of N,N-Diethyl-3-methylbenzamide (DEET) from Oil-in-Water Emulsions Stabilized by Cationic Nanocellulose and Silica Nanoparticles. Journal of the Brazilian Chemical Society, 0, , .	0.6	0